Journal of Analytical and Applied Pyrolysis 177 (2024) 106312

Contents lists available at ScienceDirect

Journal of Analytical and Applied Pyrolysis

journal homepage: www.elsevier.com/locate/jaap

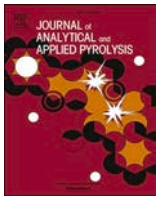

Effect of oxygen on the temperatures and conversion of tobacco in an electrically heated system

M. Bechikhi [a], F. Quilès [b], R. Lainé [a], Y. Le Brech [a], A. Dufour [a,*]

[a] Université de Lorraine, CNRS, LRGP, F-54000 Nancy, France
[b] Université de Lorraine, CNRS, LCPME, F-54000 Nancy, France

ARTICLE INFO

Keywords:
Tobacco
Electrically heated tobacco system
Pyrolysis
Oxidation
Calorimetry

ABSTRACT

The goal of Heated Tobacco products (HTPs) is to devolatilize nicotine from the tobacco by a controlled electrical heating without inducing combustion and to thereby reduce the formation of harmful and potentially harmful compounds typically related to self-sustained combustion of tobacco as in conventional cigarettes. Here, we have instrumented a commercial puffing machine and an HTP with a micro-positioning system of a thin thermocouple (0.25 mm). The puffing was conducted under N_2 or air. We provide the evolution of temperature as a function of time during standard puffing cycles and along the radial position within the tobacco plugs of tobacco sticks used as part of an electrically heated tobacco system (EHTS) during operation. The temperature profiles are nearly the same for the two atmospheres showing only minor influences of oxygen (maximum temperatures: 318 °C in air, 308 °C in N_2, at the end of the puffing cycle). The thermal degradation of the tobacco remains always globally endothermic due to the high flow rate of the cold air flowing the tobacco during the puffing. To better understand the differences between air or N_2 puffing, we have imaged the solid residues collected in the tobacco plugs by FTIR spectroscopy. The residues are clearly differentiated whatever their radial positions between air or N_2 by principal component analysis of the FTIR spectra. This result highlights similar surface oxidation phenomena of the solid residue independent of the positions. Moreover, analysis of the FTIR spectra indicates that the heating of the tobacco in the EHTS is relatively uniform along the electrically-controlled heater without signs of local hot spots. These experiments were also completed by calorimetry of tobacco upon pyrolysis or oxidation, in a 3D sensor and under a fixed bed configuration (not in the EHTS). We evidence significant exothermic phenomena from about 230 °C mainly due to gas-phase oxidation of primary volatiles in the hot gas stream. During the operation of the EHTS, such potential exothermicity is counter-balanced by strong heat losses and the high flow rate of cold air flowing through the tobacco bed during the puffing. This leads to the observed net endothermic degradation of tobacco during EHTS operation.

1. Introduction

The impact of cigarette smoke on human health is an important societal topic. Cigarette smoke leads notably to an increased incidence of various pulmonary or cardiovascular diseases [1,2]. The harmful and potentially harmful constituents (HPHC) emitted in cigarette smoke have been extensively characterized and for a long time [3]. More than 8000 chemical compounds have been identified in cigarette smoke [3] with more than 100 identified HPHCs [4]. Among them, PAH (polycyclic aromatic hydrocarbons) have been especially highlighted as important HPHCs [2,5].

Most of the HPHCs are formed at the high temperatures (up to 950 °C) induced by the smoldering combustion of tobacco in conventional cigarettes [1]. For this reason, heated tobacco products (HTPs) [6] have been developed in order to reduce and to better control the temperature of tobacco by avoiding combustion. HTPs have been marketed like Glo developed by British American Tobacco or IQOS by Philip Morris International. The goal of such HTPs is to devolatilize nicotine from the tobacco by a controlled electrical heating without inducing combustion and to thereby reduce the formation of HPHCs typically related to the self-sustained combustion of conventional cigarettes. The emissions from such HTPs have been extensively studied [7–10] and reviewed [11] but the origin of certain HPHCs detected in HTP emissions (such as PAHs) is still debated [11].

* Corresponding author.
E-mail address: anthony.dufour@univ-lorraine.fr (A. Dufour).

https://doi.org/10.1016/j.jaap.2023.106312
Received 29 September 2023; Received in revised form 13 December 2023; Accepted 15 December 2023
Available online 19 December 2023

In their recent review, Uguna and Snape [11] notably highlighted the following important remark: "Despite the evidence that IQOS heats to no more than 350 °C, there is uncertainty over the maximum temperatures reached in heat sticks and local hot spots could cause the formation and release of species, such as phenol/cresols and polycyclic aromatic compounds (PAHs)…".

This present article exactly intends to address this important point about the temperature profiles and potential hot spots during HTPs operation. Our goal is to carefully assess the operating temperatures and the effect of oxygen on the thermal degradation of tobacco in HTPs during product operation.

The effect of temperature and oxygen on tobacco conversion has been already extensively studied [12–21] but not yet on the temperature profiles in HTPs.

Wójtowicz et al. [13] have produced an important reference on the formation kinetics of the main primary volatiles from tobacco based on TGA-FTIR analysis.

Torikai et al. [14] have presented an interesting study on the effect of temperature and atmosphere (N_2 or air) on the formation of some main HPHCs. They have used a quartz tube heated by an infrared image furnace to heat tobacco plugs at 17 °C/s up to 300, 500, 800 and 1000 °C (5 s holding time at the final temperature). This study is an excellent basis to understand HPHCs formation, but the heating conditions are too different than the ones occurring in HTPs (too low holding time, too fast heating rate, etc.). Therefore, this study must be complemented by different controlled conditions closer to the ones occurring in the HTPs.

Senneca et al. [18,19] have comprehensively studied the mass loss kinetics (in TGA) and heat of reactions (by DSC) of various tobaccos as a function of the atmosphere (He, 2%vol. or 5%vol. O_2) and heating rates (5–20 °C/min). These authors clearly show a moderate effect of oxygen on mass loss and on heats of reactions for temperature lower than 400 °C. These authors have also studied the composition of volatiles by direct on-line mass spectrometry (MS) (connected to the TGA) [19]. This work was conducted in TGA (in a crucible) and it may be of interest to complete this work on entire tobacco plugs, with a flow-through of the carrier gas to promote the mass transfers (notably of O_2) within the tobacco plugs.

Paschke et al. [20] have studied the qualitative formation of main volatiles by Py-GC/MS under air or He of various tobacco additives between 350 and 1000 °C. They provided a comprehensive but qualitative analysis of volatiles and with different mass and heat transfers in the used micro pyrolyser than in an HTP.

Concerning the analysis of the solid residue ("char" or ashes), Sharma et al. [22] have studied the effect of temperature and 5%vol. O_2 on the composition of chars (by SEM, NMR and FTIR) produced in a sample boat between 200 and 700 °C. These authors highlighted the continuous decrease in OH groups with temperature and the increase of aromatic moieties up to about 600 °C. They present a comprehensive study on the chemical moieties in chars but the effect of air at temperatures of interest for HTP (< 350 °C) was not targeted and pointed out.

Concerning the temperatures analysis in HTPs, Cozzani et al. [10] have shown that the tobacco material touching the heater surface of the IQOS reaches a maximum temperature of 320 °C. Already at 0.2 mm from the heater surface, the temperature of the tobacco material was reduced to below 250 °C. The temperatures in the EHTP during its use have been confirmed by another group [23].

Despite all these numerous and extensive studies, the effect of oxygen on the thermal conversion of tobacco under suited conditions for HTPs remains unclear. Consequently, this article intends to complete the literature by showing the effect of O_2 under controlled thermal conditions relevant for HTPs. In this work, detailed temperature measurements under air and nitrogen are carried out in the tobacco during product operation.

To the best of our knowledge, this work is the first one to present the following points:

1) Puffing cycles were conducted under air or N_2 to show the effect of O_2 on the temperature profile inside the tobacco plug in a commercial HTP within a modified puffing machine;
2) The solid residue was sampled in the tobacco plug after the puffing cycles and its chemical composition was analyzed by FTIR imaging and statistical analysis;
3) The effect of oxygen on the heats of reactions is presented for the first time by using a fixed bed of tobacco with a flow-through of the gas in a 3D-sensor calorimeter.

In this work, we unravel the effect of oxygen on the temperatures during product operation and on the chemistry of solid residues (by FTIR).

2. Material & methods

2.1. Tobacco materials and EHTS

HEETS sticks (Amber type) were used as representative samples of cast-leaf tobacco typically used in HTPs. Amber HEETS were bought in tobacco stores in Nancy (France) in 2022. Their references are provided in the supplementary material (table S1). This commercial product has been previously characterized. It is composed of tobacco powder, water, glycerol, guar gum and cellulose fibers [10]. The composition is publicly available and presented in supplementary material. It has a crimped structure that we have preserved for all our experiments, including those in the fixed-bed reactor where the tobacco plug was extracted from the tobacco sticks.

The tobacco sticks were stored and conditioned for at least 48 h at 22 ± 1 °C and 60 ± 3% relative humidity prior to use.

A commercial EHTS device (IQOS® marketed by Philip Morris International) was used and bought in Nancy (2022). This EHTS has been presented in details elsewhere [10]. Briefly, the EHTS device contains a ceramic-based heating blade (heater) that heats the tobacco from the center of the tobacco plug radially outwards. Heat is supplied to the tobacco for a fixed period of 360 s heating cycle. The temperature profile of the heater is electrically controlled. During puffing, air enters the EHTS through a gap and is convected through the tobacco plug (Fig. 1), then the air and the volatiles are cooled down and carried out through the mouth piece.

2.2. Temperature analysis inside the EHTS

The scope was to accurately control the vertical position of thermocouple and by keeping a controlled vertical alignment along the same hottest point (at 4.7 mm from the tip, Fig. 1). For this purpose, we have reconstructed the IQOS device in 3D in a CAD software (supplementary material) in order to determine the accurate position of the hole and of the thermocouple for machining the IQOS device. The detailed design is presented in supplementary material. Fig. 1 presents a scheme of the device.

This system enables a good alignment in a tubing sheath of the thermocouple (very thin of 0.25 mm), a tight connection and a mechanical rigid assembly of the whole system inside a Borgwaldt commercial puffing cabinet (LM4E).

The temperature inside the tobacco was measured at different positions (starting with new stick for each position) under N_2 (purity: 5.0) or air (purity: 5.0) at 5 radial distances from the heated lamella: 0, 0.2, 0.5, 1.7, 3.4 mm. The sequence was the following: 1) introduction of the tobacco stick into the IQOS device, 2) perforating the tobacco plug with rigid metallic spindle of 0.4 mm (through the tubing sheath), 3) positioning the tobacco stick and IQOS in the puffing machine, 4) micro-positioning of the thermocouple at the targeted radial position, 5) closing and purging the cabinet, 6) puffing sequence.

Under N_2, the %vol.O_2 was always lower than 0.5%vol. as measured by the cell (provided by Borgwaldt) at the outlet of the cabinet (see video

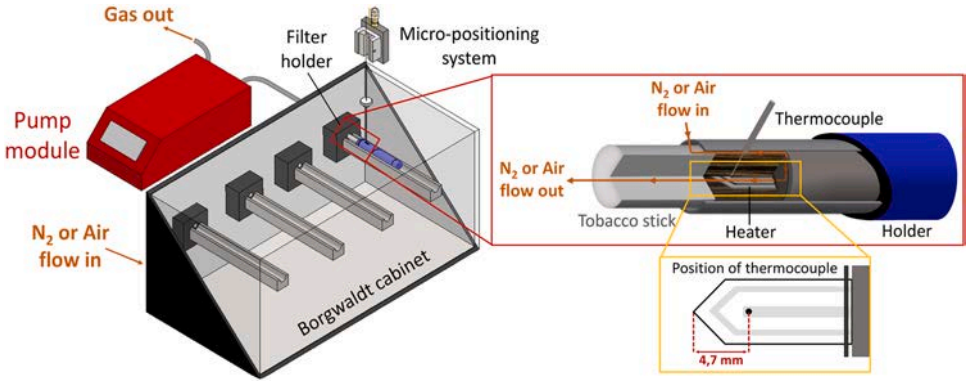

Fig. 1. Implementation of the micro-positioning system inside the puffing machine.

provided in supplementary material).

For all temperature measurements, we kept the same puffing profile (Health Canada Intense (HCI) regimen): 12 puff, 55 mL puff volume, 2 s puff duration and 30 s puff frequency.

2.3. FT-IR micro-spectroscopy of tobacco solid residue and Multivariate Data Analysis

The tobacco sticks after being used in the puffing machine under air or N_2 (but without a thermocouple to avoid its hole) were sectioned according to the radial or longitudinal direction (Fig. 2). The stick was sectioned at the axial position of the hottest point of the lamella with a Teflon mold positioned at the place of the heating lamella (Fig. 2). This Teflon mold enables to maintain the structure of the crimped tobacco plug and it is used as the reference (0 mm radial position) for the FTIR imaging. The method for the longitudinal sectioning of the plug is presented in the supplementary material.

Spectra in reflectance mode were recorded between 4000 and 800 cm^{-1} on a Bruker Vertex 70v spectrometer equipped with a Hyperion 2000 microscope and a × 15 objective controlled by the OPUS 7.5 software. A KBr beam splitter and a MCT detector were used. The resolution of the single beam spectra was 4 cm^{-1}. Masks of 200 μm × 200 μm were used to record the spectra. The size of the mask was chosen to get enough energy at the detector in order to record reliable spectra with good signal-to-noise ratios. The number of bidirectional double-sided interferogram scans was 400. All interferograms were Fourier processed using the power phase correction and a Blackman-Harris three-term apodization function. Measurements were performed at 21 ± 1 °C in an air-conditioned room. Water vapour subtraction was performed when necessary, and baseline was corrected at 1900 and 900 cm^{-1} before further analysis of the spectra. The FT-IR spectra were recorded with a name code highlighting their radial position (in mm from the lamella) or longitudinal position, the different zone in the plug (see Fig. 3) and the gas used during the product operation (air or N_2).

Multivariate analysis was performed using the Unscrambler V12.2 software. Principal component analysis (PCA) was applied to FT-IR spectra in the fingerprint spectral range of 1900–900 cm^{-1}. We have followed the pioneering work of Nimlos et al. [24] which was proposed on wood chars. These authors have clearly shown the potential interest of FT-IR imaging of chars to assess their "local" chemistry, which is well related to their thermal history. This methodology was not yet applied to tobacco chars as a function of temperature and O_2. Our group has previously shown the interest of PCA to differentiate pyrolysis regimes or biomass composition [25–27].

2.4. Tobacco fixed bed analysis by calorimetry

In order to better understand the effect of O_2 on the conversion of tobacco, we have developed a calorimeter under fixed bed configuration. The calorimeter measures the sensible heat (heating of tobacco and of char), phase change (evaporation) and the heat of reactions (bond breaking, crosslinking, oxidation, etc.). It is a suitable technique to understand the effect of O_2 on the thermochemical conversion of tobacco by measuring the exo- or endo-thermic phenomena under controlled thermal conditions.

Fig. 4 presents the scheme of the developed set-up. It is based on a Setaram DSC111 calorimeter (Caluire, France) which has been modified with tailored quartz tubes (including a sintered plate). The quartz tubes must have an accurate machining and positions to allow a good control and reproducibility of the calorimeter signal.

The calorimeter has been calibrated by the fusion of pure metals. The mass of the tobacco bed (30 mg) has been optimized in order to avoid a saturation of our signal (notably during gas-phase oxidation reactions) and to get a good signal during pure pyrolysis conditions. The structure of the crimped tobacco inside the quartz tube has been kept. A flow rate (20 mL/min at 20 °C, Patm.) of the carrier gas (Argon or 1%vol. O_2) was controlled by mass flow controllers (Brooks) and injected through the crimped tobacco bed. This is of tremendous importance to control mass transfers through the crimped tobacco because they highly impact

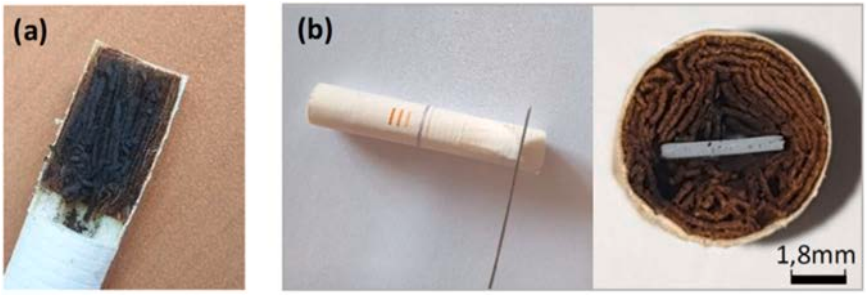

Fig. 2. Longitudinal (a) and radial (b) sections of tobacco sticks with the Teflon mold positioned in lieu of the heating lamella.

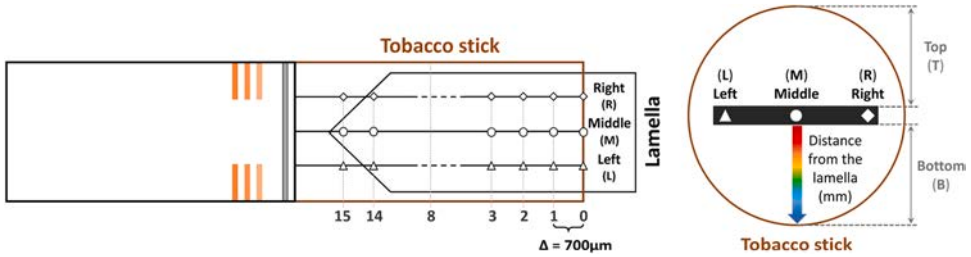

Fig. 3. Position of the different FT-IR measuring points in the tobacco stick in the longitudinal and radial sections.

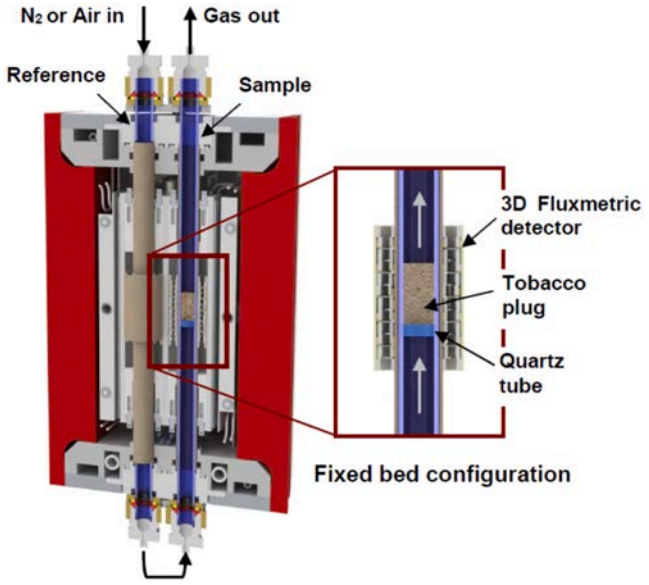

Fig. 4. Scheme of the calorimeter used to conduct pyrolysis and oxidation of tobacco under fixed bed configuration, designed at CNRS Nancy, and based on a Setaram (France) calorimeter.

pyrolysis and oxidation reactions. The temperature program was: 1200 s at 20 °C, then 10 °C/min up to 500 °C, 10 min at 500 °C. We have conducted experiments with 1%vol. O_2 to better control the exothermicity similarly as Senneca et al. [18] or Sharma et al. [22].

3. Results

3.1. Temperature profiles in the EHTS

The evolutions of temperatures in the tobacco plug heated by the IQOS device and during a puffing cycle are presented in Fig. 5. These evolutions are the average of 5 independent experiments (all raw results are provided in supporting material).

The temperatures in the tobacco plug on the heated lamella (at a radial position of 0 mm) occurring during a puffing cycle in air are in good agreement with the ones previously measured by Cozzani et al. [10] with a decreasing temperature during the puffs and a maximal temperature of 318 °C at the final puff. Our temperature of the first puff is slightly lower (250 °C) in our case. It is important to notice that for each position, the temperatures decrease of about 50 °C during the puff due to the important cooling effect of cold gas for both N_2 and air. Therefore, we did not notice combustion of the tobacco (global exothermic phenomena) during the puffs in the HTPs under air.

The temperatures measured in this work are higher (still under air) than the ones presented by Cozzani et al. [10] at 0.2 mm maybe due to different accuracies of the thermocouple micro-positioning systems. The setup used for the temperature measurements in Cozzani et al. [10] was not presented in detail. The purpose of this present work is notably to acquire the temperature at high precision by a micro-positioning system (design fully presented in this article).

To the best of our knowledge, this study is the first one to present the evolution of temperatures in the tobacco during a puffing cycle conducted both under air and N_2. The measured temperatures under N_2 are about 10–20 °C lower than in air, for all radial positions (unless for 0.5 mm).

In order to better compare the 2 atmospheres (air and N_2), the temperatures were corrected by the density and thermal conductivity of these 2 gases. Indeed, the pump imposed a volumetric flow within the tobacco plug. Therefore, the volumetric heat capacity of the gases may impact the heat transfers by forced convection within the plugs. The corrected temperatures are individually compared for each radial position for air and N_2 in the supporting material.

The corrected temperature profile is close to be the same for all positions between the two atmospheres, as shown in Fig. S5. Moreover, the same thermal behaviour upon puffing is observed, with a similar re-covery time after puffs highlighting that O_2 does not lead to internal thermal run away.

Only a slight difference in the corrected temperature may be observed, where the corrected temperature is slightly lower on the heating source (at 0 mm radial position, on the heated lamella) under N_2 due to some potential mass transfers hindrance of the gas (air and pyrolysis volatiles) on the tobacco material in contact with the lamella compared to within the crimped structure of the tobacco plug. We were not able to explain why the corrected temperatures are similar at 0.5 mm for both air and N_2. The slight difference in the corrected temperatures in the tobacco between the two atmospheres may result from some gas-phase oxidation of volatiles under air as evidenced by calorimetry (see the next section). Such reactions may occur at temperatures higher than about 230 °C (based on calorimetry) and this heating source may increase the overall temperature within the whole tobacco plug, even at radial position of 1.7 and 3.4 mm, by radial heat transfers and air flow uneven distribution within the crimped structure. Another potential concurrent mechanism may be the heterogeneous reaction of O_2 on the tobacco surface, even at low temperatures, as it is highlighted in the next section on FTIR analysis, where weak oxidation effects independent of the temperature are observed.

3.2. FT-IR micro-spectroscopy of solid residues produced during the puffs and PCA analysis

After puffing cycles in air or N_2 (without thermocouples), we have sampled the solids (tobacco/char) remaining in the tobacco plugs of the sticks. Then the solids were carefully sectioned at the hottest radial positioned (as explained in material and methods).

Fig. 6 presents the sectioned tobacco plugs with typical FTIR spectra obtained as a function of their position along the radial position.

Our spectra are consistent with those published by Sharma et al. [22] and Zhu et al. [28] up to 350 °C but with different resolutions due to our different FTIR techniques (KBr pellets in their cases).

The main FTIR peaks are highlighted in Fig. 6 and their tentative assignment are given in Table 1 [22,24,28,29].

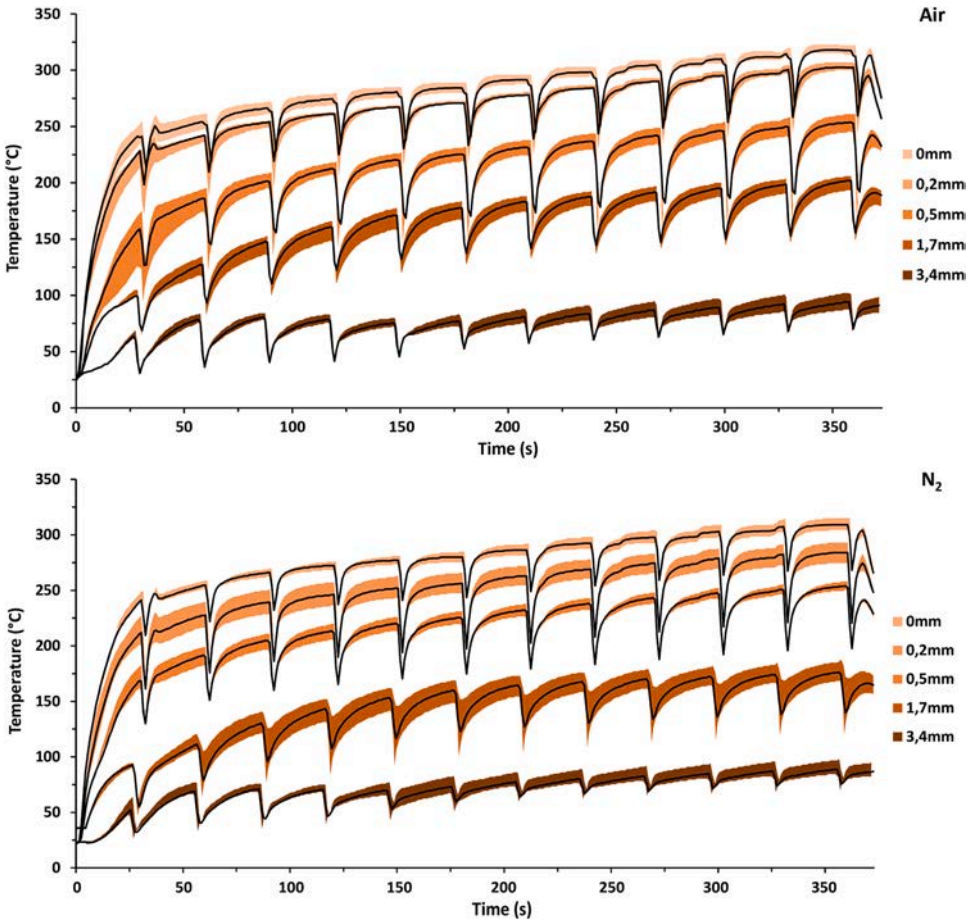

Fig. 5. Comparison between temperature measured under Air and N_2 at five different positions from the heater lamella: 0, 0.2, 0.5, 1.7 and 3.4 mm. The curve represents the average of 5 replicates, and the coloured region indicates the range between the maximum and minimum temperatures. The raw measured data are provided as supplementary material.

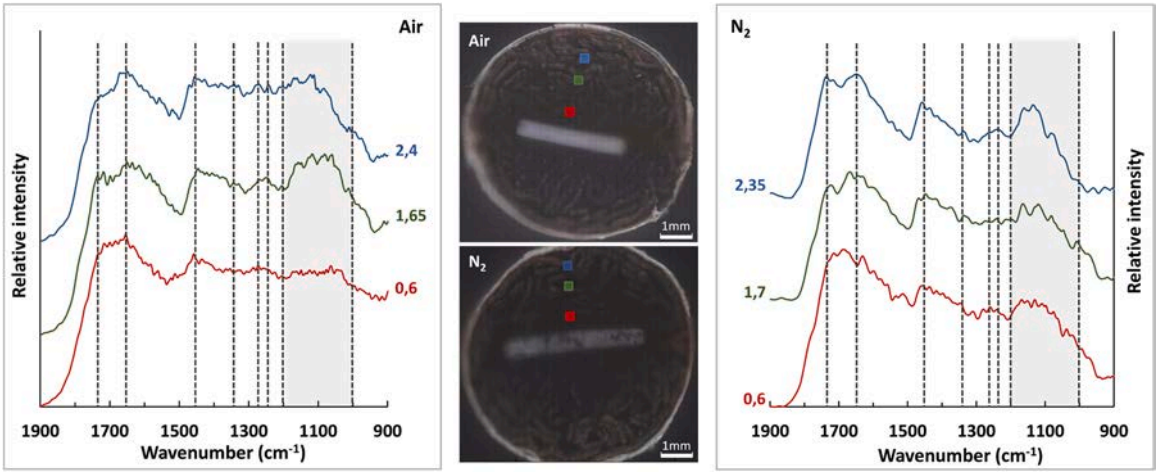

Fig. 6. Visible images of a radial section of tobacco stick heated under air or nitrogen with the areas outlining the FT-IR measurement regions (200 μm * 200 μm) at different distances from the lamella (mm).

Two regions of the spectra, i.e. 1800–1500 and 1200–1000 cm^{-1}, are highly impacted by the heating in presence or not of O_2. Region 1500–1800 cm^{-1}, mainly assigned to C═O and aromatic bonds, are less defined with the increase of the temperature. Under nitrogen, the bands at ~1740 cm^{-1} assigned to C═O from esters are stable for spectra recorded. The shape of the spectra changes in region 1700–1600 cm^{-1}, the bands originating from the vibration modes of C═O bonds in hemicelluloses are degraded upon heating. It is in relationship with the spectral features between 1200 and 1000 cm^{-1}, mainly assigned to the carbohydrate moiety. Indeed, the features of the bands in this region change drastically only at 0.6 mm from the lamella, the hottest area of the stick.

As the temperature increases (along the radial position, closer to the lamella), the complexity of the spectrum decreases for both N_2 and air

Table 1
Assignments of main FTIR bands.

Region (cm^{-1})	Tentative assignment
1790	Lactone ?
1740 – 1750	νC=O ester
~1700	νC=O phenolic ester, ketons, aldehydes
1650 – 1680	νC=O aryl
1620 – 1640	νC =C, δH_2O of adsorbed water
1590	νC=C aromatic in lignin
1500	νC=C aromatic
1450	δCH_2
1400 – 1475	δCH_n
1370	δC-H
1360	δC-OH
1310 – 1360	Skeletal vibrations C-C and C-O
1274; 1240	νC-O in lignins
1000 – 1200	νC-O, νC-OH, νC-O-H, νC-C

treatment but with a more pronounced effect for air treatment (see Fig. 6, spectra at 0.6 mm). But the spectra are still complex, and it was not possible to assign all bands due to bands overlap.

For this reason, we have conducted a multivariate analysis using principal component analysis (PCA) in the fingerprint spectral range 1900–900 cm^{-1}.

Figs. S7 and S8 in supporting material show the score plot of the principal component 1 (PC-1) against the principal component 2 (PC-2). These two components account for up to 70% of the variability in the spectra with mainly PC-1 as the major contribution. PC-1 and PC-2 are presented in supporting material.

It is clear from Figs. S7 and S8 that the points are well clustered along PC-1 as a function of their radial position for both N_2 or air: from the right (hottest point closer to the lamella) to the left (coldest position). Their PC-1 both exhibit a higher contribution for higher temperatures from bands at 1030 cm^{-1} (C-C, C-C-O or C-C stretching) and of C-O and C-C stretching as markers of the thermal conversion [22,24].

Then we have treated all the FTIR spectra from all radial positions for N_2 and air together in order to highlight a potential difference between air and N_2. We have analyzed 2 different sticks (both for air and N_2, therefore a total of 4 sticks) heated in 2 different puffing experiments to validate that the differences between the spectra did not come from the puffing experiment itself but by the carrier gas.

Fig. 7 presents the PCA analysis for all the spectra.

It is important to notice that PC-1 explains more than 82% of the variance and that the spectra obtained by air or N_2 are clearly separated whatever their radial positions. This means that even at low temperatures, air presents a significant effect on the chemical structure of heated tobacco compared to N_2. The oxidative effect of O_2 on the surface of the tobacco material is not dependent on the radial position and is therefore not linked to temperature-dependent oxidation reactions. To validate this result, we have heated the tobacco plugs in a fixed bed reactor (presented in supporting material) at 150 °C under N_2 or air. The PCA results presented in supplementary material confirms the findings that air presents a significant effect on solid composition even for temperatures as low as 150 °C. A GC/MS analysis (presented in the supplementary material) of the volatiles (trapped in methanol at the outlet of the fixed bed) did not reveal different markers under air or N_2, confirming that gas-phase reactions are not importantly impacted by air at this temperature.

In order to better understand the main differences between the spectra, the typical spectra (located at the same radial positions and highlighted in Fig. 7) are presented in Fig. 8.

The spectra from the "air" regime clearly presents a pattern of a more "carbonized" char [22,24] with less resolved C-O, C-C and C=O bands and an important contribution in C=C bands. PC-1 is presented in Fig. 9 and clearly depicts that the bands at 1140–1170 cm^{-1} (assigned to C-OH and C-O stretching) are more preserved in the case of N_2 as well as the ones at 1740–1790 cm^{-1} (C=O stretching). In the case of air, C=C (potentially in aromatic structures of solid residues) and C-O-C rather contribute to PC-1.

In Fig. 9, bands promoted under N_2 absorb at 1790, 1740, 1450, 1170 and 1140 cm^{-1}. They are assigned to C=O stretchings of lactone and esters, CH_2 stretchings, and C-C and C-O stretchings from carbohydrates. This result shows a higher stability of these moieties under this N_2 regime. Conversely, a band absorbing at 1700 cm^{-1} and a broad band absorbing between 1500 and 1600 cm^{-1} are promoted under air conditions. They are the result of changes in the C=O bonds and the aromatic moieties. This result can be interpreted by the conversion of hemicelluloses. Indeed, it has been shown that hemicelluloses decomposition occurs earlier than that of cellulose due to less stable moieties [24].

We have also investigated if "hot spots" could be clearly differentiated between air and N_2 by PCA of FTIR spectra along the longitudinal

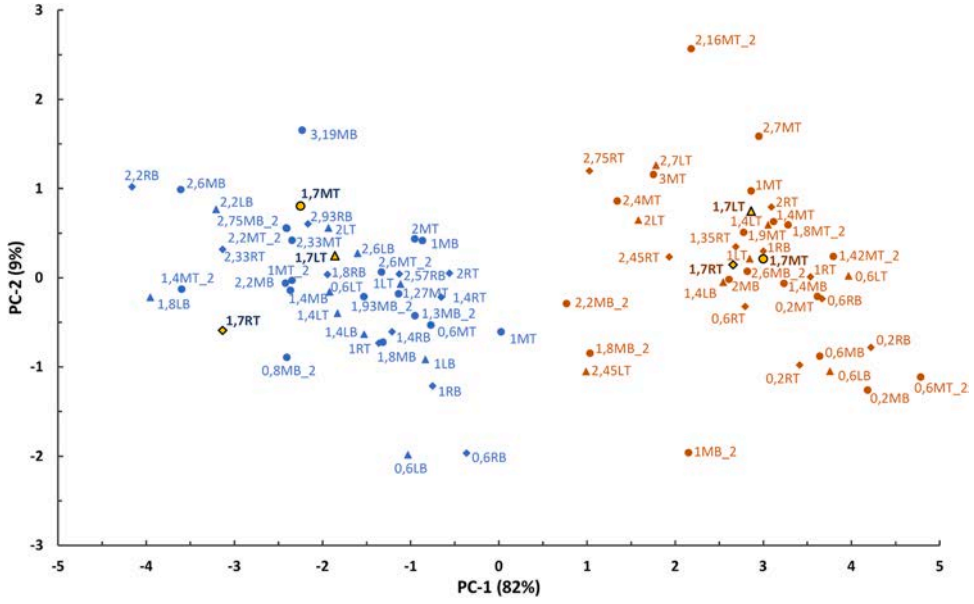

Fig. 7. PCA of FT-IR spectra of the radial section of tobacco stick puffed under air (orange points) and N_2 (blue points) with replicate points for both air and N_2, the spectra of the highlighted points are presented in Fig. 8.

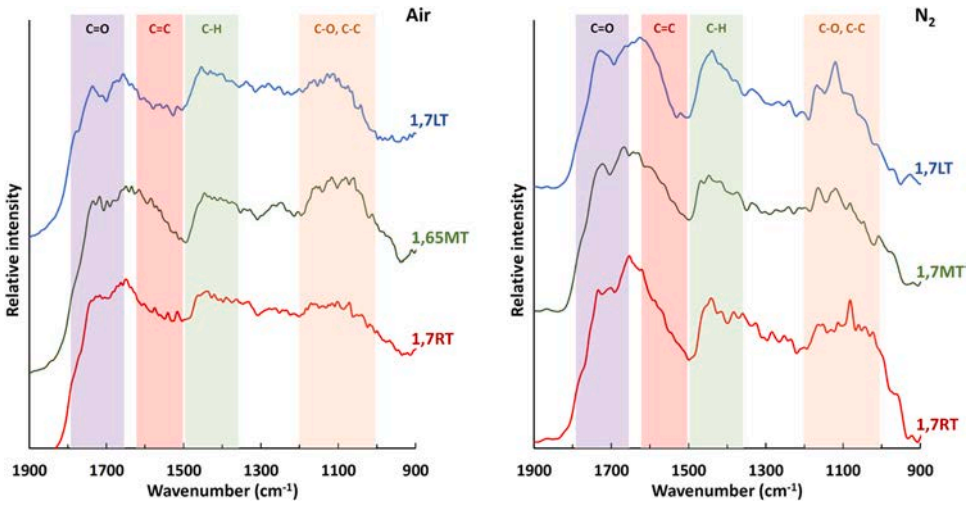

Fig. 8. Typical spectra depicting the "air" regime and the "N_2" regime, at the same radial positions.

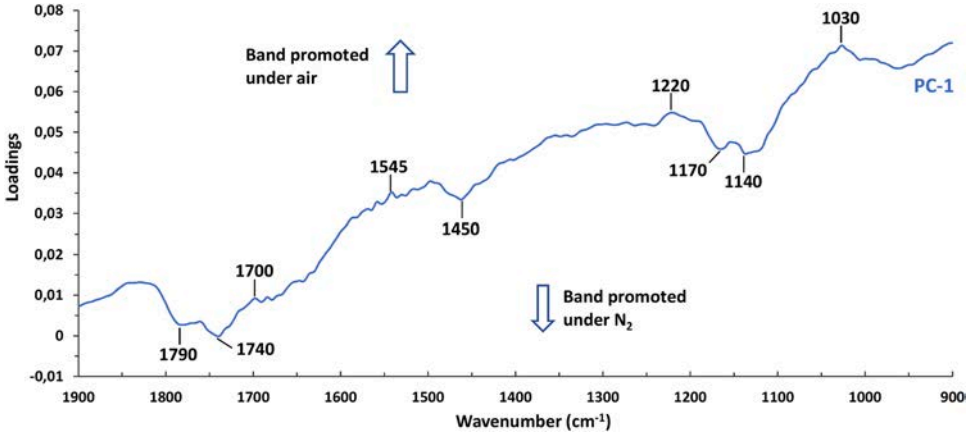

Fig. 9. Score loading plots for PC-1 from PCA analysis of radial section of tobacco stick operated under air and N_2.

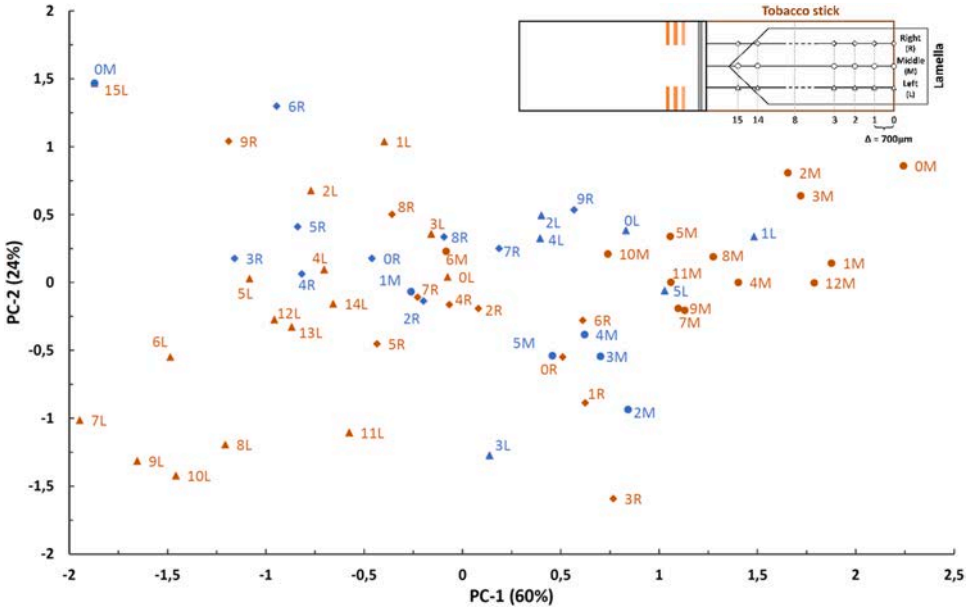

Fig. 10. PCA of FT-IR spectra of longitudinal section of tobacco sticks puffed under air (orange points) and N_2 (blue points).

direction on the leaf of tobacco in contact with the heated lamella (Fig. 10).

The Fig. 10 clearly shows that the FTIR spectra between air and N_2 are not clearly differentiated probably due to mass transfers hindrance leading to a bad contact between the carrier gas and tobacco leaf in contact to the heated lamella. Furthermore, there is no hot spots observed (both under air or N_2) that can be clearly differentiated by the PCA.

3.3. Calorimetry of tobacco thermal conversion

In order to better understand the potential oxidation mechanisms occurring on tobacco during the EHTS operation, we have carried out DSC experiments in a flow-through fixed bed configuration. This configuration allows to control and to promote the mass transfers between air (or N_2) and the tobacco surface.

The reproducibility of the DSC signals is presented in supporting material. Fig. 11 presents the results obtained in the fixed bed calorimeter under different conditions.

Concerning the thermal degradation of tobacco under inert conditions (argon atmosphere), a first endothermal signal is evidenced at around 100 °C (drying) and then a second endothermal signal occurs between 130 and 250 °C probably due to the evaporation of nicotine and glycerol, the evaporation of other volatile products present in the tobacco and to endothermic decomposition of hemicelluloses and pectin [18,30]. Then the pyrolysis is globally athermic with very low enthalpy of reactions in agreement with Senneca et al. [18] who has studied the thermicity of tobacco pyrolysis in a different DSC configuration (in a crucible). The heat of reactions during biomass pyrolysis highly depends on the mineral content and notably of potassium [31,32]. The mineral content of the tobacco has been analyzed in this present work and it is presented in the supplementary material. The high content of minerals (notably of potassium) in the tobacco explains the global athermic signal obtained during the cellulose pyrolysis in the range 300–350 °C. Indeed, we have previously shown [31] that potassium promotes crosslinking reactions and therefore the exothermic signal during cellulose pyrolysis. The endothermic phenomena occurring during bonds scissions is overlapped by exothermic phenomena (crosslinking, bonds formation) leading to a global athermic pyrolysis of cellulose. A similar mechanism stands for lignin pyrolysis [33].

The heat flow signal from thermal degradation of tobacco under an oxidative atmosphere presents a much more intense signal than under the non-oxidative atmosphere. The first endothermal signal is still present, but its importance is overwritten by important exothermic phenomena as the temperature increases. A first exothermic phenomenon occurs between 300 °C and 400 °C followed by a second stronger exothermic signal from 400 up to 500 °C (Fig. 11). One can notice that the beginning of the curve is similar between the non-oxidative and oxidative conditions but from about 230 °C, the signal for the oxidative condition deviates from the signal of the non-oxidative condition towards exothermic phenomena. This shows that exothermic phenomena are detected from 230 °C by calorimetry under this fixed bed configuration. This result is in agreement with the ones of Senneca et al. [18] but our calorimeter presents a higher sensitivity, because it is composed by a 3D sensor (of more than a hundred of thermocouples) and our configuration in a fixed bed under constant flow rate enhances the mass transfers of O_2 in the tobacco bed and the oxidation phenomena. Our configuration is more representative to the flow-through regime occurring during tobacco puffing than the crucible configuration used by Senneca et al. [18] but due to its constant flow of pre-heated gas in the fixed-bed configuration it still remains fundamentally different than the conditions in HTPs during puffing. These results are obtained for our given conditions with a constant flowrate of gas flowing through the tobacco sample in a reactor (the calorimeter) with minimal heat losses to the environment. This thermal condition is fundamentally different during EHTS operation, which involves puffing with a higher flow rate of gas (cooling down the tobacco as analyzed in the previous section), non-uniform heating, and heat losses. A higher volume fraction of O_2 (e.g. 21%vol. instead of 1%vol.) in the carrier gas would not change the starting temperature of the exothermal phenomena as previously shown by Senneca et al.[18] but it would increase the intensity of the exothermal peak.

In order to better understand the 2 exothermic peaks, we have further oxidised the tobacco char produced by the thermal degradation of tobacco under the non-oxidative environment within the calorimeter. The char was kept inside the calorimeter after the thermal degradation, cooled down under Argon, and re-heated under 1%vol. O_2 flow. It is interesting to notice that the heterogeneous oxidation of char in the fixed bed reactor starts before 400 °C (Fig. 11). The work of Senneca et al. [18] revealed the oxidation of char after 400 °C at a temperature slightly higher than in our case due to our enhanced mass transfers of O_2.

Therefore, the first exothermal peak occurring between 230 and 400 °C during thermal degradation of tobacco under oxidative conditions may be mainly attributed to the gas-phase oxidation of the pyrolysis volatiles. The second peak after 400 °C can be attributed to the heterogeneous oxidation ("combustion") of the char.

Although the thermal and mass transfers conditions are different in the calorimeter than in the EHTS, these results are useful to propose an explanation to the slightly higher corrected temperatures obtained during EHTS operation in air which may be attributed to gas-phase oxidation reactions.

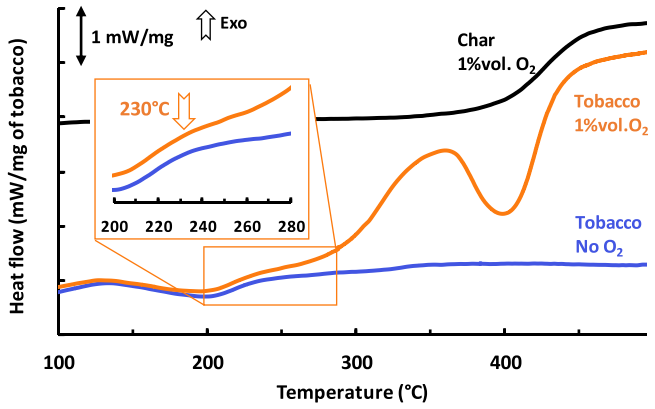

Fig. 11. Comparison between the calorimetry signals for thermal degradation of tobacco under inert (non-oxidative) and oxidative atmospheres and char (produced after tobacco pyrolysis in the calorimeter) under an oxidative atmosphere in a fixed bed configuration.

4. Conclusion

In this work, we have intended to understand the thermal conditions and the influence of O_2 on the thermal conversion of tobacco in an EHTS during a standard puffing sequence.

For this purpose, the temperature profile in the tobacco stick during its heating by the EHTS device and during puffing was measured using a thin thermocouple positioned at different radial positions in the tobacco plug by a micro-positioning system under both air and N_2 atmospheres. The maximum temperature under air is reached at the end of the puffing cycle and reaches about 320 °C and the temperature decreased during the puffs, showing a net endothermic behaviour. These temperatures analyses are in agreement with published data [10,23]. The measured temperature in the tobacco plug under air is about 10 to 20 °C higher than under N_2. When normalizing the measured temperatures with the volumetric heat capacity of the carrier gas to remove the influence of the thermophysical properties of the carrier gas, it is found that the corrected temperature profiles are close to be the same for all positions between the two atmospheres and that the same thermal behaviour

upon puffing with a similar recovery time after puffs is observed for the two atmospheres. We clearly evidence that, even if some exothermic degradation phenomena may occur during operation in the EHTS, the thermal degradation of the tobacco is net endothermic as any potential exothermic phenomena is always counter-balanced by the cold high flowrate of air and heat losses to the environment due to the strong thermal gradients in the tobacco plug during heating. Therefore, the temperature is always reduced during the puffs demonstrating that there is no combustion occurring during product operation.

The solid residues (heated tobacco and chars) obtained after the puffing cycles were analyzed by FTIR spectroscopy. A statistical analysis clearly reveals that all the solids heated under air can be discriminated from the ones heated under N_2 whatever their radial position and temperature condition in the tobacco plug. This means that air impacts the chemical structure of the solid residue even at temperatures as low as 150 °C. The effect of oxygen on the solid residue is not influenced by the temperature within the temperature range occurring in the EHTS during operation. This result demonstrates that this observed effect of oxygen is not linked to combustion of the tobacco as the effect is independent of the temperature. The longitudinal FTIR results also show that there is no indication of hotspots on the solid residue in contact with the heated lamella, showing that the heating of the tobacco along the electrically-controlled heater is relatively uniform.

Finally, we have also studied the thermal conversion of tobacco in a fixed bed calorimeter. In this experimental setting, exothermic reactions were observed from 230 °C under air probably from the gas-phase oxidation of primary volatiles. Therefore, gas-phase oxidation of primary volatiles may also occur during the operation of the EHTS but these reactions do not lead to global exothermic phenomena. During EHTS operation and the puffing, any potential exothermic reaction contributing to the thermal degradation is overwritten by heat losses and the cooling effect of the high flow rate of cold air during puffing, which leads to a net global endothermal phenomena. Net exothermic phenomena were not evidenced even between the puffs when stagnating air is present in the tobacco plug.

The comprehensive analysis of the thermal conditions occurring in the tested EHTS during operation presented in this work show that the thermal degradation of the tobacco is net endothermic, largely independent of oxygen, and that combustion of the tobacco does not occur. Moreover, analysis of the degraded tobacco indicates that there are no hotspots in the tobacco during heating and that oxygen effects of the tobacco is shown to be independent of the temperature condition in the EHTS tobacco stick.

The methodology proposed in this work can be used to study the pyrolysis and oxidation of all other biomasses or solid materials. Especially the FTIR imaging method could be useful to map the chemical composition of solid residues produced in all other lab-scale or industrial scale thermochemical reactors, for instance as to understand biochar heterogeneity produced in pyrolysis reactors. Finally, the fixed bed calorimeter is of potential interest for the pyrolysis community to better unravel the enthalpy of pyrolysis reactions (for various solid materials) and to study oxidation reactions under well-controlled mass transfer conditions.

CRediT authorship contribution statement

Manon Bechikhi: conducted all experiments and calibration, processed the data. Fabienne Quilès: analyzed and discussed the FTIR data. Richard Lainé : developed the micropositioning system. Yann Le Brech: supervised the laboratory experiments, calorimetry calibration. Anthony Dufour: project administration, designed the study, discussed the data and wrote the article.

Declaration of Competing Interest

The authors declare the following financial interests relationships which may be considered as potential competing interests: Anthony DUFOUR group reports financial support was provided by Philip Morris International Research and Development Campus Neuchâtel.

Data Availability

The raw data are provided as supplementary material and could be published as a supplementary material.

Acknowledgement

Philip Morris International is the sole source of funding and sponsor of this research. MB, FQ and AD thank J. Grausem from the spectroscopies and microscopies facility (SMI) of LCPME (UMR 7564, Université de Lorraine – CNRS, 405, rue de Vandoeuvre, 54600 Villers-lès-Nancy, France, https://lcpme.ul.cnrs.fr).

Appendix A. Supporting information

Supplementary data associated with this article can be found in the online version at doi:10.1016/j.jaap.2023.106312.

References

[1] R.R. Baker, Smoke generation inside a burning cigarette: modifying combustion to develop cigarettes that may be less hazardous to health. Prog. Energy Combust. Sci. 32 (2006) 373–385, https://doi.org/10.1016/j.pecs.2006.01.001.
[2] United States Surgeon General. The Health Consequences of Smoking – 50 Years of progress: A Report of the Surgeon General: (510072014–001) 2014. https://doi.org/10.1037/e510072014–001.
[3] A. Rodgman, T.A. Perfetti, Boca Raton. The Chemical Components of Tobacco and Tobacco Smoke, CRC Press, 2008, https://doi.org/10.1201/9781420078848.
[4] W.H. Organization, The Scientific Basis of Tobacco Product Regulation: Report of a WHO Study Group, World Health Organization, 2007.
[5] A. Rodgman, Studies of polycyclic aromatic hydrocarbons in cigarette mainstream smoke: identification, tobacco precursors, control of levels: a review, Contrib. Tob. Nicotine Res. 19 (2001) 361–379, https://doi.org/10.2478/cttr-2013-0724.
[6] Flora J., Digard H., Sinclair C., Belushkin M., International P.M. Heated Tobacco Products (HTPs): Standardized Terminology and Recommendations for the Generation and Collection of Emissions 2020:11.
[7] M.R. Smith, B. Clark, F. Lüdicke, J.-P. Schaller, P. Vanscheeuwijck, J. Hoeng, et al., Evaluation of the Tobacco Heating System 2.2. Part 1: description of the system and the scientific assessment program, Regul. Toxicol. Pharmacol. 81 (2016) S17–S26, https://doi.org/10.1016/j.yrtph.2016.07.006.
[8] J.-P. Schaller, D. Keller, L. Poget, P. Pratte, E. Kaelin, D. McHugh, et al., Evaluation of the Tobacco Heating System 2.2. Part 2: chemical composition, genotoxicity, cytotoxicity, and physical properties of the aerosol, Regul. Toxicol. Pharmacol. 81 (2016) S27–S47, https://doi.org/10.1016/j.yrtph.2016.10.001.
[9] M. Forster, S. Fiebelkorn, C. Yurteri, D. Mariner, C. Liu, C. Wright, et al., Assessment of novel tobacco heating product THP1.0. Part 3: Comprehensive chemical characterisation of harmful and potentially harmful aerosol emissions, Regul. Toxicol. Pharmacol. 93 (2018) 14–33, https://doi.org/10.1016/j.yrtph.2017.10.006.
[10] V. Cozzani, F. Barontini, T. McGrath, B. Mahler, M. Nordlund, M. Smith, et al., An experimental investigation into the operation of an electrically heated tobacco system, Thermochim. Acta 684 (2020), 178475, https://doi.org/10.1016/j.tca.2019.178475.
[11] C.N. Uguna, C.E. Snape, Should IQOS emissions be considered as smoke and harmful to health? A review of the chemical evidence, ACS Omega 7 (2022) 22111–22124, https://doi.org/10.1021/acsomega.2c01527.
[12] R.R. Baker, A review of pyrolysis studies to unravel reaction steps in burning tobacco, J. Anal. Appl. Pyrolysis 11 (1987) 555–573, https://doi.org/10.1016/0165-2370(87)85054-4.
[13] M.A. Wójtowicz, R. Bassilakis, W.W. Smith, Y. Chen, R.M. Carangelo, Modeling the evolution of volatile species during tobacco pyrolysis, J. Anal. Appl. Pyrolysis 66 (2003) 235–261, https://doi.org/10.1016/S0165-2370(02)00116-X.
[14] K. Torikai, S. Yoshida, H. Takahashi, Effects of temperature, atmosphere and pH on the generation of smoke compounds during tobacco pyrolysis, Food Chem. Toxicol. 42 (2004) 1409–1417, https://doi.org/10.1016/j.fct.2004.04.002.
[15] T. McGrath, R. Sharma, M. Hajaligol, An experimental investigation into the formation of polycyclic-aromatic hydrocarbons (PAH) from pyrolysis of biomass materials, Fuel 80 (2001) 1787–1797, https://doi.org/10.1016/S0016-2361(01)00062-X.
[16] T.E. McGrath, W.G. Chan, M.R. Hajaligol, Low temperature mechanism for the formation of polycyclic aromatic hydrocarbons from the pyrolysis of cellulose, J. Anal. Appl. Pyrolysis 66 (2003) 51–70, https://doi.org/10.1016/S0165-2370(02)00105-5.
[17] T.E. McGrath, J.B. Wooten, W. Geoffrey Chan, M.R. Hajaligol, Formation of polycyclic aromatic hydrocarbons from tobacco: The link between low temperature

residual solid (char) and PAH formation, Food Chem. Toxicol. 45 (2007) 1039–1050, https://doi.org/10.1016/j.fct.2006.12.010.
[18] O. Senneca, R. Chirone, P. Salatino, L. Nappi, Patterns and kinetics of pyrolysis of tobacco under inert and oxidative conditions, J. Anal. Appl. Pyrolysis 79 (2007) 227–233, https://doi.org/10.1016/j.jaap.2006.12.011.
[19] O. Senneca, S. Ciaravolo, A. Nunziata, Composition of the gaseous products of pyrolysis of tobacco under inert and oxidative conditions, J. Anal. Appl. Pyrolysis 79 (2007) 234–243, https://doi.org/10.1016/j.jaap.2006.09.011.
[20] M. Paschke, C. Hutzler, F. Henkler, A. Luch, Oxidative and inert pyrolysis on-line coupled to gas chromatography with mass spectrometric detection: on the pyrolysis products of tobacco additives, Int. J. Hyg. Environ. Health 219 (2016) 780–791, https://doi.org/10.1016/j.ijheh.2016.09.002.
[21] Y. Peng, X. Hao, Q. Qi, X. Tang, Y. Mu, L. Zhang, et al., The effect of oxygen on in-situ evolution of chemical structures during the autothermal process of tobacco, J. Anal. Appl. Pyrolysis 159 (2021), 105321, https://doi.org/10.1016/j.jaap.2021.105321.
[22] R.K. Sharma, J.B. Wooten, V.L. Baliga, P.A. Martoglio-Smith, M.R. Hajaligol, Characterization of char from the pyrolysis of tobacco, J. Agric. Food Chem. 50 (2002) 771–783, https://doi.org/10.1021/jf0107398.
[23] S. Uchiyama, M. Noguchi, N. Takagi, H. Hayashida, Y. Inaba, H. Ogura, et al., Simple determination of gaseous and particulate compounds generated from heated tobacco products, Chem. Res Toxicol. 31 (2018) 585–593, https://doi.org/10.1021/acs.chemrestox.8b00024.
[24] M.-K. Bahng, B.S. Donohoe, M.R. Nimlos, Application of an fourier transform-infrared imaging tool for measuring temperature or reaction profiles in pyrolyzed wood, Energy Fuels 25 (2011) 370–378, https://doi.org/10.1021/ef101312a.
[25] L. Jia, Y. Le-Brech, B. Shrestha, M.B. Frowein, S. Ehlert, G. Mauviel, et al., Fast pyrolysis in a microfluidized bed reactor: effect of biomass properties and operating conditions on volatiles composition as analyzed by online single photoionization mass spectrometry, Energy Fuels 29 (2015) 7364–7374, https://doi.org/10.1021/acs.energyfuels.5b01803.
[26] L. Jia, F. Buendia-Kandia, S. Dumarcay, H. Poirot, G. Mauviel, P. Gérardin, et al., Fast pyrolysis of heartwood, sapwood, and bark: a complementary application of online photoionization mass spectrometry and conventional pyrolysis gas chromatography/mass spectrometry, Energy Fuels 31 (2017) 4078–4089, https://doi.org/10.1021/acs.energyfuels.7b00110.
[27] L.Y. Jia, M. Raad, S. Hamieh, J. Toufaily, T. Hamieh, M.M. Bettahar, et al., Catalytic fast pyrolysis of biomass: superior selectivity of hierarchical zeolites to aromatics, Green. Chem. 19 (2017) 5442–5459, https://doi.org/10.1039/C7GC02309J.
[28] L. Zhu, J. Xu, Y. Dai, J. Jiang, S. Liao, G. Zhou, et al., Mechanism study of tobacco pyrolysis based on the analysis of characteristic products and in-situ identification of functional groups evolution on pyrolytic char, J. Anal. Appl. Pyrolysis 167 (2022), 105681, https://doi.org/10.1016/j.jaap.2022.105681.
[29] B. Richard, F. Quilès, C. Carteret, O. Brendel, Infrared spectroscopy and multivariate analysis to appraise α-cellulose extracted from wood for stable carbon isotope measurements, Chem. Geol. 381 (2014) 168–179, https://doi.org/10.1016/j.chemgeo.2014.05.010.
[30] J.L. Torero, J.I. Gerhard, M.F. Martins, M.A.B. Zanoni, T.L. Rashwan, J.K. Brown, Processes defining smouldering combustion: integrated review and synthesis, Prog. Energy Combust. Sci. 81 (2020), 100869, https://doi.org/10.1016/j.pecs.2020.100869.
[31] Y. Le Brech, T. Ghislain, S. Leclerc, M. Bouroukba, L. Delmotte, N. Brosse, et al., Effect of potassium on the mechanisms of biomass pyrolysis studied using complementary analytical techniques, ChemSusChem 9 (2016) 863–872, https://doi.org/10.1002/cssc.201501560.
[32] C.D. Blasi, A. Galgano, C. Branca, Exothermic events of nut shell and fruit stone pyrolysis, ACS Sustain. Chem. Eng. 7 (2019) 9035–9049, https://doi.org/10.1021/acssuschemeng.9b01474.
[33] B. Shrestha, Y. le Brech, T. Ghislain, S. Leclerc, V. Carré, F. Aubriet, et al., A multitechnique characterization of lignin softening and pyrolysis, ACS Sustain. Chem. Eng. 5 (2017) 6940–6949, https://doi.org/10.1021/acssuschemeng.7b01130.